

**Vortex fluctuations in high- $T_c$  thin films close to the resistive transition**

Örjan Festin and Peter Svedlindh

*Department of Materials Science, Uppsala University, P. O. Box 534, SE-751 21 Uppsala, Sweden*

Fredrik Rönning and Dag Winkler

*Quantum Device Physics Laboratory, Department of Microtechnology and Nanoscience, Chalmers University of Technology, SE-412 96 Göteborg, Sweden*

(Received 15 December 2003; revised manuscript received 5 April 2004; published 21 July 2004)

Flux noise and ac susceptibility measurements have been performed on epitaxial  $\text{YBa}_2\text{Cu}_3\text{O}_7$  films to investigate dynamical properties of vortex fluctuations close to the resistive transition. The validity of the fluctuation-dissipation theorem is verified by the proportionality between flux noise and ac susceptibility results. The zero-field flux-noise spectrum  $[S_\phi(f)]$  can be characterized as follows. Below a temperature dependent frequency  $f_0(T)$ , the flux noise spectrum is frequency independent. For frequencies  $f > f_0(T)$ , the flux noise spectrum follows  $f^{-x}$ , with  $x \approx 1.5-1.75$ . The characteristic frequency  $f_0$  exhibits a dramatic decrease close to the resistive transition;  $f_0$  decreases by 3–4 orders of magnitude in a temperature interval of  $\Delta T \approx 1$  K. Moreover, the flux noise spectrum scales as  $fS_\phi = g(f/f_0(T))$ , where  $g(\cdot)$  is a scaling function. The influence of a weak perturbing magnetic field ( $H_{dc}$ ) on the characteristics of the flux noise spectrum has been investigated. While the general characteristics of the flux noise spectrum remain, except for a change in frequency dependence at  $f > f_0$ , the characteristic frequency  $f_0$  exhibits a dramatic increase with increasing applied field;  $f_0$  increases by 3–4 orders of magnitude on increasing the field from zero to a few oersteds. Moreover, it is found that  $f_0$  is proportional to  $H_{dc}^y$ , with  $y \approx 1.15$ . The results are interpreted in terms of thermally generated vortex-antivortex fluctuations in combination with fluctuations of field-generated vortices.

DOI: 10.1103/PhysRevB.70.024511

PACS number(s): 74.78.Bz, 74.40.+k, 74.25.Ha

**I. INTRODUCTION**

Thermally created vortex fluctuations drive the zero-field phase transition of Kosterlitz-Thouless (KT) type between the superconducting and normal states in thin film superconductors as well as in two-dimensional (2D) Josephson junction arrays.<sup>1</sup> Much of the experimental work have been performed in zero field using two-coil mutual inductance,<sup>2-4</sup> flux-noise,<sup>2,3,5,6</sup>  $I$ - $V$ , and resistance<sup>7,8</sup> measurements to characterize the dynamical properties of vortex fluctuations close to the transition. The evidence of 2D vortex fluctuations in the case of high- $T_c$  superconductors is particularly convincing for  $\text{BiSrCaCuO}$ ,<sup>2</sup> which in comparison with  $\text{YBa}_2\text{Cu}_3\text{O}_{\delta-7}$  (YBCO) exhibits a much larger anisotropy. However, YBCO also shows, in a narrow temperature range, a behavior characteristic of 2D vortex fluctuations.<sup>3</sup> In fact, even for bulk YBCO single crystals, which exhibit a three-dimensional (3D)  $XY$ -like transition to the zero-resistance state, experimental<sup>9</sup> as well as theoretical<sup>10,11</sup> results indicate a decoupling of the  $\text{CuO}_2$  planes at a temperature just above the transition temperature, and a behavior at higher temperatures dominated by 2D vortex fluctuations.

Much less work have been devoted to vortex fluctuations in the presence of a magnetic field applied perpendicular to the superconducting film or the 2D Josephson junction array. The vortex physics will in this case be complicated by the coexistence of thermally and field created vortices. Early experiments performed on superconducting films<sup>12</sup> were affected by pinning effects masking some of the intrinsic behavior of the vortex medium. More recent experiments performed on a weakly frustrated triangular array of Josephson junctions,<sup>13</sup> at temperatures much below the zero-field

KT transition temperature where the vortex pinning is weak, reveal that the vortex dynamics is different from Drude's classical description.<sup>1</sup> The frequency dependence of the vortex dynamics instead indicates that the vortex mobility vanishes logarithmically in the limit of small frequencies, a feature pointing to anomalously slow vortex diffusion. Simulations on the 2D  $XY$  model using time-dependent Ginzburg-Landau dynamics and including weak perpendicular magnetic fields<sup>14,15</sup> are in accordance with the experimental results obtained in Ref. 13. Moreover, the simulations were performed in a large temperature interval, describing the behavior of the vortex dynamics at temperatures both below and above the zero-field KT transition.

In the present paper, we report a detailed study of the frequency dependence of the vortex dynamics in weak applied perpendicular magnetic fields and at temperatures close to the zero-field resistive transition for thin YBCO films. The experimental results, which were obtained from two-coil mutual inductance and flux-noise measurements covering a wide range of frequencies, indicate a strongly temperature and field dependent characteristic frequency of the vortex dynamics.

**II. EXPERIMENT**

The thin film samples used in the present work are square shaped ( $5 \times 5$  mm<sup>2</sup>) 200 Å and 500 Å thick  $\text{YBa}_2\text{Cu}_3\text{O}_{7-\delta}$  films grown on  $\text{SrTiO}_3$  (STO) substrates by pulsed laser deposition.<sup>16</sup> The 500 Å thick YBCO film is capped with a 200 Å thick Au layer. From the strong correlation between the  $T_c$  and  $\Delta T_c$  values and the crystallinity of YBCO films, as

previously seen,<sup>16</sup> the films are expected to be highly *c*-axis oriented and with only YBCO [100](001)||STO [100](001) in-plane orientation.

The experimental setup is a system based on a dc superconducting quantum interference device (SQUID) designed for two-coil mutual inductance and flux-noise measurements.<sup>17,18</sup> The solenoid used in the mutual inductance measurements has a diameter of 3 mm. Inside this solenoid is a concentrically mounted pick-up coil, wound as a first order gradiometer and having a diameter of 1.2 mm. The face of this coil set is approximately 500  $\mu\text{m}$  back from the superconducting film surface. The frequency dependent conductance  $G(\omega, T)$  is determined by inversion of the ac susceptibility  $\chi(\omega, T)$ , which is measured using a model 7260 DSP lock-in amplifier from EG&G Instruments, following the procedure outlined in Ref. 19. The flux-noise spectrum  $S_\phi(\omega)$  is determined by standard Fourier analysis of the SQUID signal in the absence of ac magnetic fields using a HP 35670A dynamic signal analyzer. The dynamic signal analyzer was also used to measure higher harmonics of the magnetization in response to ac magnetic fields of different amplitudes. The sample space is magnetically shielded by  $\mu$  metal and niobium cans, giving a residual dc magnetic field of approximately 2 mOe. After mounting of a superconducting film sample, the sample was not removed from the shielded environment until both ac susceptibility and flux-noise measurements had been completed. The dc magnetic field is created by a superconducting Helmholtz coil, operated in persistent mode. The SQUID system noise is approximately  $2 \times 10^{-5} \phi_0/\text{Hz}^{1/2}$  and  $7 \times 10^{-6} \phi_0/\text{Hz}^{1/2}$  at 1 Hz and 100 Hz, respectively, independent of the dc magnetic field for the range of fields used in the present work ( $H_{dc} \leq 3$  Oe).

The zero-field-cooled (ZFC) magnetization is measured by cooling the sample to a low temperature in the absence of a field, turning on a dc magnetic field, and measuring the magnetization in this field as the sample slowly warms through the superconducting transition temperature. The field-cooled (FC) magnetization is next obtained by slowly cooling the sample in the same dc magnetic field and measuring the magnetization as the sample slowly cools.

### III. RESULTS

Figure 1(a) shows the temperature dependence of the out-of-phase component of the ac susceptibility  $\chi''(T)$  in zero applied dc magnetic field for the 500  $\text{\AA}$  thick YBCO film. The frequency of the ac magnetic field was 1.7 Hz and the different curves correspond to different ac field amplitudes. Figure 1(b) shows the Fourier-transform spectrum  $|M(f)|$  of the magnetization response to a 5.1 Hz ac field at  $H_{dc} = 0$  Oe and at a temperature close to where  $\chi''(T)$  exhibits its largest magnitude, while Fig. 1(c) shows the corresponding results for  $H_{dc} = 1$  Oe. The onset of a nonlinear response in zero applied dc magnetic field occurs approximately for an ac field amplitude of  $H_{ac} = 0.5$  mOe, while the nonlinear response in superimposed dc magnetic field occurs at slightly larger ac field amplitudes; for  $H_{dc} = 1$  Oe, the onset occurs in the field range 1–3 mOe. One interesting observation is that

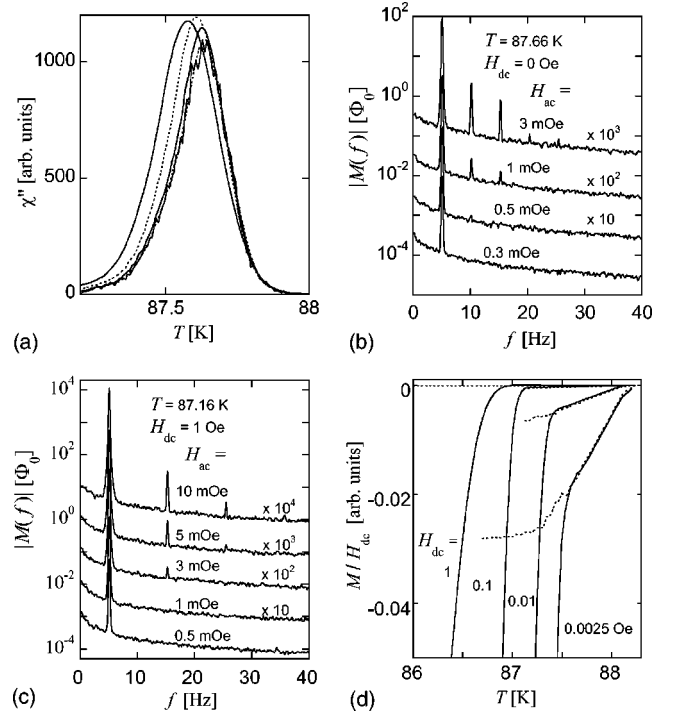


FIG. 1. (a)  $\chi''$  versus temperature: the different curves correspond to different amplitudes of the ac magnetic field; left to right 10 mOe (solid line), 3 mOe (dashed line), 1 mOe (solid line), 0.3 mOe (dashed line), and 0.1 mOe (solid line).  $H_{dc} = 0$  Oe and  $f = 1.7$  Hz. (b) Fourier-transform spectra of the magnetization response to a 5.1 Hz ac magnetic field.  $H_{dc} = 0$  Oe. (c) Fourier-transform spectra of the magnetization response to a 5.1 Hz ac magnetic field.  $H_{dc} = 1$  Oe. (d) ZFC (solid line) and FC (dashed line) susceptibility versus temperature. The different curves correspond to different dc field amplitudes. 500  $\text{\AA}$  thick film.

in zero applied dc magnetic field one detects even harmonics of similar magnitude to the magnitude of the odd harmonics, while the even harmonics are suppressed in a dc magnetic field of  $H_{dc} = 1$  Oe. This observation will not be further discussed, since the emphasis here is on the linear response of the vortex system. Measurements of  $|M(f)|$  at other temperatures and ac field frequencies gave similar results for the onset of a nonlinear response of the vortex system. All results to be presented below were obtained in the linear response regime, using an ac field amplitude of  $H_{ac} = 0.3$  mOe.

Figure 1(d) shows the ZFC and FC susceptibilities ( $M/H_{dc}$ ) versus temperature; the ZFC and FC susceptibilities have been normalized with the ZFC susceptibility value corresponding to complete screening. The magnetization curves corresponding to  $H_{dc} = 2.5$  mOe were measured by cooling the sample in a compensating dc magnetic field to reduce the residual field in the experimental setup to be of order 0.1 mOe. The irreversibility temperature  $T_{irr}(H_{dc})$  is defined from the temperature where the ZFC and FC susceptibility curves merge. For temperatures  $T \geq T_{irr}(H_{dc})$ , the vortex system is in thermodynamic equilibrium and the sample contains a uniform density of vortices. Moreover, in the FC state it is seen that the sample is almost completely penetrated by the applied field. The ac susceptibility and flux-noise mea-

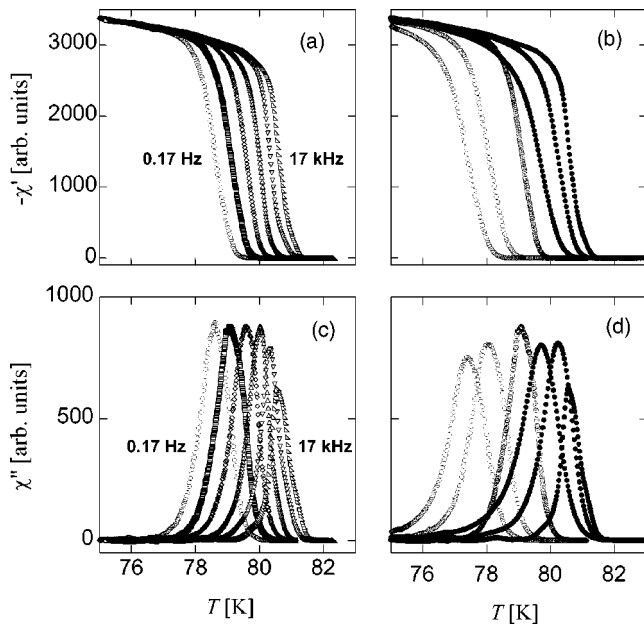


FIG. 2. (a)  $\chi'$  and (c)  $\chi''$  versus temperature: the different curves correspond to different frequencies of the ac magnetic field; left to right 0.17 Hz, 1.7 Hz, 17 Hz, 170 Hz, 1.7 kHz, and 17 kHz. (b)  $\chi'$  and (d)  $\chi''$  versus temperature for two different frequencies of the ac magnetic field; open and filled circles correspond to 1.7 Hz and 17 kHz, respectively. The different curves correspond to different dc magnetic fields  $H_{dc}$ ; from left to right  $H_{dc}=1$  Oe,  $H_{dc}=0.1$  Oe, and  $H_{dc}=0$  Oe. 200 Å thick film.

measurements discussed below were performed on a vortex system corresponding to the FC state. In fact, the flux-noise measurements were performed at temperatures corresponding to  $T \geq T_{irr}(H_{dc})$ , implying that comparisons between ac susceptibility and flux-noise results correspond to this temperature range.

### A. ac susceptibility and ac conductance

In Fig. 2, the real [Figs. 2(a) and 2(b)] and imaginary [Figs. 2(c) and 2(d)] parts of the ac susceptibility  $\chi = \chi' - i\chi''$  are shown versus temperature for the 200 Å thick film. The imaginary part of the ac susceptibility in zero field [Fig. 2(c)] reveals for each frequency of the ac field a well-defined dissipation peak, but there is a tendency that  $\chi''(T)$  decreases in magnitude and broadens for larger frequencies. This we take as evidence of sample heterogeneity, yielding a broadening of the features in the ac susceptibility for large frequency (temperature), while this broadening gradually disappears with decreasing frequency (temperature). The effect of a perpendicular applied magnetic field is visualized in Figs. 2(b) and 2(d), where it is shown for two different frequencies of the ac magnetic field that the characteristic features of the ac susceptibility are suppressed to lower temperature with increasing magnetic field. It is also possible to distinguish a slight broadening of the features in  $\chi(T)$  with increasing magnetic field.

In Fig. 3, the zero-field ac conductance  $\omega G$  is shown versus temperature for the 200 Å thick [Fig. 3(a)] and 500 Å

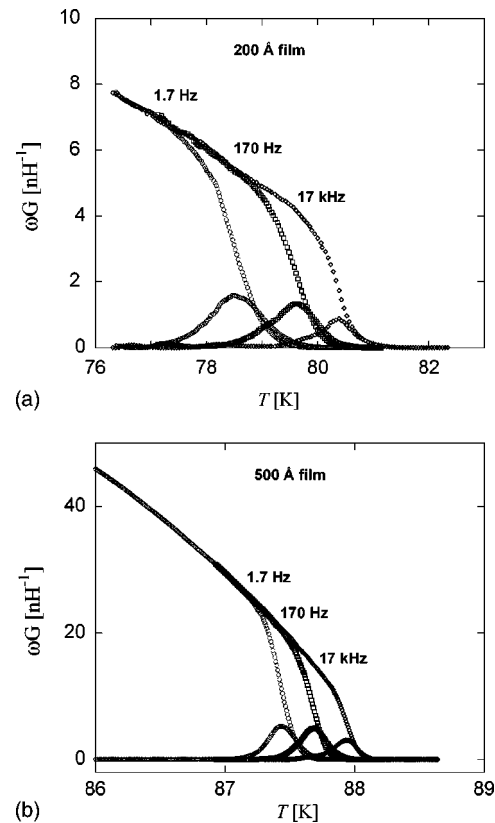


FIG. 3. ac conductance  $\omega G$  versus temperature. The different curves correspond to different frequencies of the ac field.  $H_{dc} = 0$  Oe. (a) 200 Å thick film and (b) 500 Å thick film.

thick [Fig. 3(b)] YBCO films, respectively. At low temperature, where the dissipation of the superconducting film is negligible [ $\omega \text{Re}(G) = 0$ ], the behavior is that of a pure inductor characterized by  $\omega \text{Im}[G(T)] = L_k^{-1}(T)$ . Here  $L_k(T)$  is the kinetic inductance related to the effective penetration depth of the superconducting film  $\Lambda(T) = 2\lambda^2(T)/d$ , where  $\lambda(T)$  and  $d$  are the bulk penetration depth and film thickness, respectively, by  $L_k(T) = \mu_0 \Lambda(T)/2$ . Close to the mean field transition temperature, one expects that  $L_k^{-1}(T) \propto (T_{c0} - T)$ ,<sup>20</sup> in agreement with the behavior of  $\omega \text{Im}[G(T)]$  shown in Fig. 3; extrapolating the linear part of this temperature dependence to  $\omega \text{Im}(G) = 0$ , one obtains  $T_{c0} = 83.5$  K and  $T_{c0} = 88.5$  K for the 200 Å and 500 Å thick YBCO films, respectively. The ac conductance in applied dc fields yields the same value of the mean field critical temperature.

### B. Flux noise

In Fig. 4, zero-field flux-noise spectra are shown versus frequency at three different temperatures for the 200 Å thick film. The feature observed at the highest temperature for frequencies  $f < 0.1$  Hz is not related to the vortex dynamics of the sample, but originates from the heater current used in the temperature control system. The most salient features of the flux-noise spectra can be described as follows. For frequencies much larger than a temperature dependent characteristic frequency of the vortex medium  $f \gg f_0(T)$ , the flux noise

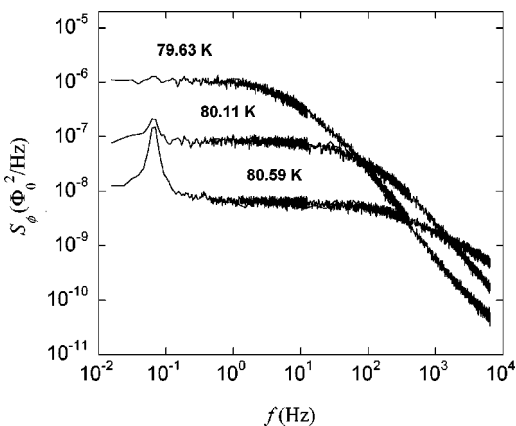
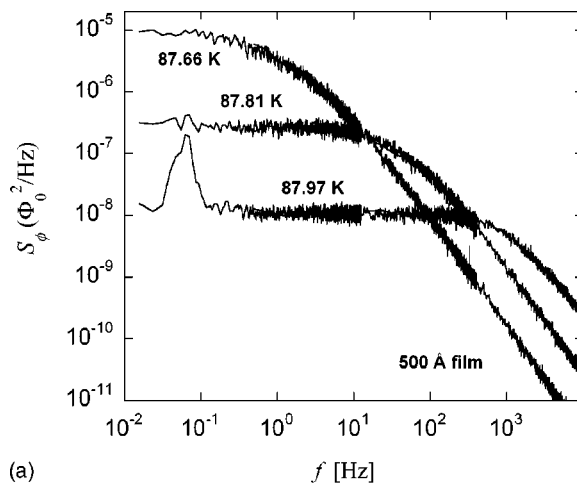


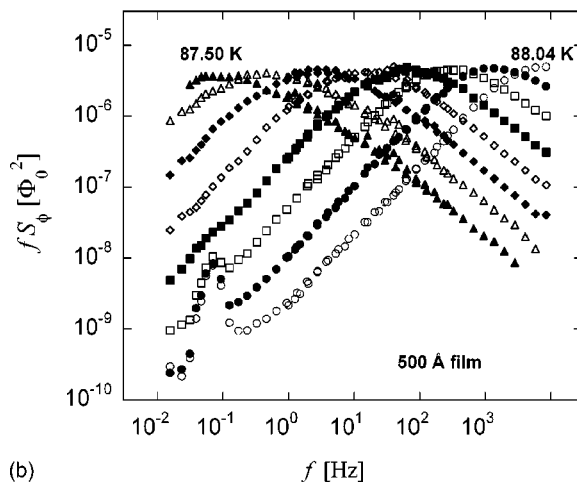
FIG. 4. Spectral density of magnetic flux noise  $S_\phi$  versus frequency for three different temperatures.  $H_{dc}=0$  Oe. 200 Å thick film.

spectrum follows a  $f^{-x}$  dependence, with  $x \approx 1.55$ . For frequencies  $f \ll f_0(T)$ , the flux-noise spectrum instead is frequency independent (white noise). At constant temperature  $T$ , the shoulder in the noise spectrum approximately defines  $f_0(T)$ . Moreover, the plateau value of a noise spectrum is proportional to the zero-frequency limit of the conductance  $G$ , which is related to the resistance as  $R=1/G$ .

The experimental setup measures the magnetic flux noise with a distance between the film surface and the pick-up coil being much larger than the relevant microscopic length, which for a superconducting film corresponds to the perpendicular penetration depth  $\Lambda$ .<sup>21</sup> In this case, the magnetic field due to the vortex medium at the position of the pick-up coil is spreading out, and the expected frequency dependence for frequencies  $f \gg f_0(T)$  corresponds to a  $f^{-x}$  dependence, with  $x=2$ .<sup>21</sup> To the best of our knowledge, this high-frequency behavior has not been observed experimentally, something that we attribute to a weak dispersion in critical temperatures caused by oxygen deficiency and thus in the characteristic time scales of the vortex medium, resulting in a  $f^{-x}$  dependence with  $x < 2$ . Moreover, at constant temperature, the heterogeneity of the sample results in a flux-noise spectrum with a transition region, between the frequency dependence of the noise spectrum in the two frequency limits  $f \gg f_0(T)$  and  $f \ll f_0(T)$ , that is broadened in frequency. In support of these claims, we show in Fig. 5(a) zero-field flux-noise spectra for the 500 Å thick YBCO film. This film is capped with a thin layer of Au, and it is therefore expected that this film should exhibit less heterogeneity with respect to oxygen concentration. For this film, the flux-noise spectra for frequencies  $f \gg f_0(T)$  exhibit a  $f^{-x}$  dependence, with  $x \approx 1.75$ . These claims are further supported by flux-noise spectra measured on a YBCO film being rather more heterogeneous,<sup>23</sup> as evidenced by the broad transition region  $\Delta T_c$  as well as the broad transition region in the flux-noise spectrum between the frequency dependence in the  $f \gg f_0(T)$  and  $f \ll f_0(T)$  frequency limits; this film exhibited a  $f^{-1}$  dependence for frequencies  $f \gg f_0(T)$ . Based on these results obtained for YBCO films of varying quality, it seems clear that the disagreement between theoretical predictions for  $S_\phi(f)$  and experimental results is to a large extent caused by imperfect sample quality.



(a)



(b)

FIG. 5. (a) Spectral density of magnetic flux noise  $S_\phi$  versus frequency for three different temperatures.  $H_{dc}=0$  Oe. 500 Å thick film. (b)  $fS_\phi$  versus frequency for eight different temperatures 88.04 K, 87.97 K, 87.89 K, 87.81 K, 87.74 K, 87.66 K, 87.58 K, and 87.50 K. The noise spectra have been smoothed by averaging over logarithmically spaced frequency segments.

Figure 5(b) shows  $fS_\phi$  versus frequency for the 500 Å thick YBCO film at eight different temperatures. In such a plot, the characteristic frequency  $f_0$  at each temperature is defined as the frequency where  $fS_\phi$  exhibits its maximum value.

Figure 6 shows flux-noise spectra versus frequency together with ac susceptibility results at both  $H_{dc}=0$  Oe and  $H_{dc}=1$  Oe for three different temperatures. The flux-noise spectrum should relate to the dissipative part of the ac susceptibility, measured in the linear response regime, as

$$S_\phi(f) \propto \frac{T\chi''(f)}{f}. \quad (1)$$

Figure 6 shows that this relation is obeyed to a high degree of precision for the present experiments, since it is possible to find a frequency and temperature independent constant that will make the ac susceptibility data overlap perfectly with the flux-noise spectra. Moreover, the relation is satisfied both in zero applied dc field and in weak dc magnetic fields



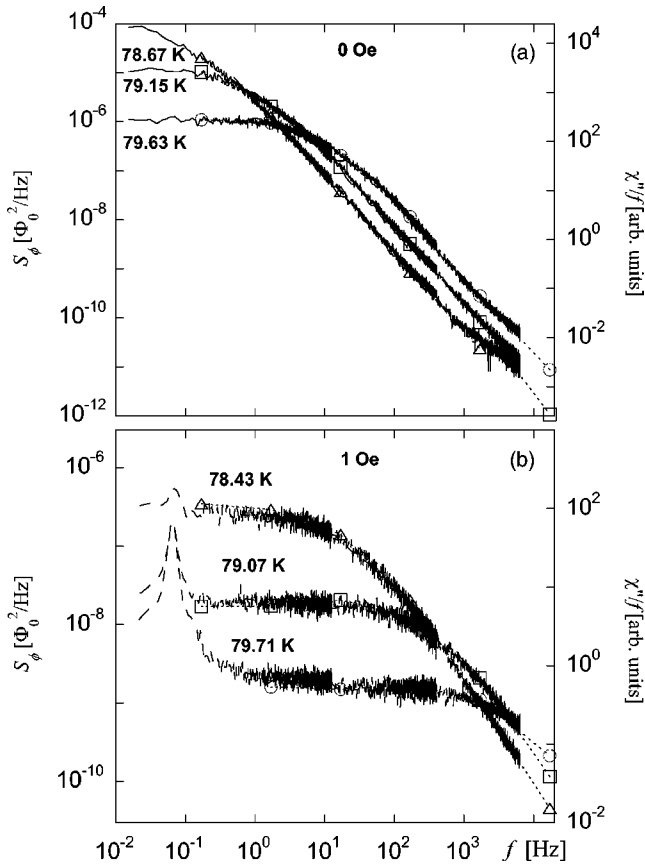


FIG. 6. Spectral density of magnetic flux noise  $S_\phi$  (left-hand scale, solid lines) and  $\chi''/f$  (right-hand scale, open symbols) versus frequency for three different temperatures. (a)  $H_{dc} = 0$  Oe and (b)  $H_{dc} = 1$  Oe. 200 Å thick film.

applied perpendicular to the sample surface. Theoretical work<sup>21,24</sup> also shows that it is possible to relate the flux-noise spectrum to the ac conductance by

$$S_\phi(f) = C(T)\text{Re}[G(f)], \quad (2)$$

where  $C(T)$  is a weakly temperature dependent constant, establishing a link between different quantities used to describe the dynamics of the vortex medium in a superconductor.

Figure 7 shows flux-noise spectra obtained at constant temperature ( $T = 79.15$  K) and for four different applied magnetic fields. The effects of a weak perpendicular magnetic field are twofold. First, the characteristic frequency increases with increasing magnetic field; compared to zero field (residual field inside the  $\mu$  metal can), the value of  $f_0$  increases by more than three orders of magnitude in a field of  $H_{dc} = 3$  Oe. Second, the plateau value of a noise spectrum decreases with increasing magnetic field; compared to zero field, the flux-noise value corresponding to the plateau decreases by more than three orders of magnitude in a field of  $H_{dc} = 3$  Oe, implying also that the zero-frequency limit of the resistance increases by more than three orders of magnitude. The increase in resistance is a natural consequence of the increase in the density of free vortices on applying a dc magnetic field to the sample. The field dependence of  $f_0$  and  $R$  will be discussed in more detail below.

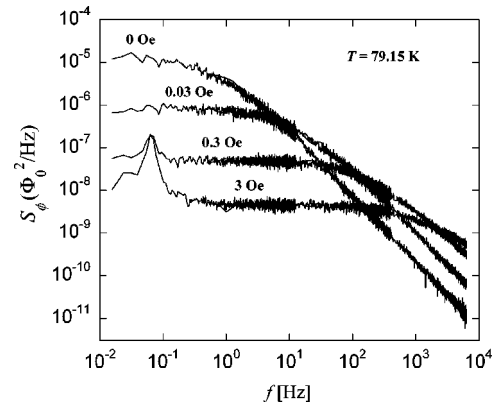


FIG. 7. Spectral density of magnetic flux noise  $S_\phi$  versus frequency for four different dc magnetic fields  $H_{dc}$ .  $T = 79.15$  K. 200 Å thick film.

#### IV. DISCUSSION

YBCO films have been studied in a temperature range just below the mean field transition temperature  $T_{c0}$ , where pinning due to ever present microscopic disorder can be kept at a low level, thus making it possible to study the intrinsic dynamical behavior of the vortex medium. However, our results indicate some type of heterogeneity in the samples, presumably due to a weak dispersion in oxygen concentration, giving rise to a likewise weak dispersion in critical temperatures and thus in the characteristic time scales of the vortex medium. The oxygen concentration in the two samples is to some extent reflected in the  $T_{c0}$  values;  $T_{c0} \approx 89$  K and  $T_{c0} \approx 83$  K for the 500 Å and 200 Å thick YBCO films, respectively. The smaller value of  $T_{c0}$  obtained for the 200 Å thick YBCO film is a combined effect due to out-diffusion of oxygen from the bare surface of the film<sup>16</sup> and finite size effects. Moreover, the influence of heterogeneity in oxygen concentration was examined, after having completed the mutual inductance and flux-noise measurements, by leaving the non-capped 200 Å thick YBCO film in vacuum and at room temperature for a period corresponding to a few days. The result was an oxygen deficient superconducting film exhibiting a decrease of the transition temperature by approximately 1 K and a significantly broadened transition region.

The general characteristics of the vortex dynamics can be understood as follows. Assuming that the vortex motion is described by a diffusion process, which considering the linear Ohmic response of the vortex system can be described as a flux flow or possibly a thermally assisted flux flow process, it is possible to relate the probing frequency  $f$  to a probing length scale  $r_f$  by  $r_f \approx (D/2\pi f)^{1/2}$ , where  $D$  corresponds to the vortex diffusion constant.<sup>22</sup> Moreover, above the resistive transition temperature, correlations between vortices are described by a temperature dependent correlation length  $\xi(T)$  that strongly increases in magnitude as the resistive transition is approached from above. In 2D and in zero applied dc magnetic field,  $\xi(T)$  corresponds to the KT correlation length, relating to the separation between a vortex and an antivortex, above which vortex correlations exponentially decay to zero. This implies that when  $r_f < \xi(T)$  (high fre-

quency), the flux-noise spectrum probes correlated vortex dynamics, while  $r_f > \xi(T)$  (low frequency) implies that uncorrelated vortex motion is probed. The crossover in length scale occurs at a frequency  $f_0$  defined by  $r_f = \xi(T)$ .

In the following, we will analyze the dynamical behavior of the vortex medium using the frequency dependence of  $fS_\phi(f)$ , which displays the same characteristic frequency dependence as  $\chi''(f)$  measured in the linear response regime. Theoretical expressions for the frequency dependent response of the vortex medium have been derived using the Coulomb gas model.<sup>1</sup> In the Coulomb gas analogy, a vortex and an antivortex correspond to Coulomb gas charges with positive and negative charge, respectively, and the frequency dependent response is given by the vortex dielectric function  $1/\epsilon(f)$ .<sup>22</sup> At high temperatures, close to but below  $T_{c0}$ , the frequency dependent response is of Drude type describing the response of free vortices,

$$fS_\phi(f) \propto \frac{(f/f_0)}{(f/f_0)^2 + 1}. \quad (3)$$

At low temperatures, close to the resistive transition, the response is expected to be dominated by bound vortex pairs (at least in zero applied dc field) and has been found to be well parametrized by the Minnhagen phenomenology (MP) form,<sup>1,2,15</sup>

$$fS_\phi(f) \propto \frac{2(f/f_0)\ln(f/f_0)}{\pi(f/f_0)^2 - 1}. \quad (4)$$

Equations (3) and (4) suggest that the noise data should scale as  $fS_\phi(f, T) = g(f/f_0(T))$ , where  $g(\cdot)$  is a scaling function, implying that noise data obtained at different temperatures should collapse onto a common curve when plotted as a function of  $f/f_0(T)$ . This prediction of scaling has been shown to apply to both Josephson junction arrays<sup>5</sup> and YBCO thin films,<sup>23</sup> even though the frequency dependence predicted for frequencies  $f/f_0(T) \gg 1$  was not observed experimentally. In Fig. 8, the prediction of scaling for zero dc magnetic field is put to test for the present two samples. For both samples, the prediction of scaling is well obeyed. Deviations from scaling may possibly be discerned for the 200 Å thick film at  $f/f_0(T) \gg 1$  for the highest temperatures included in the scaling analysis, something that we associate with the broadening observed in  $\chi''(T)$  for larger frequencies [cf. Fig. 2(c)]. Also included in this figure is the frequency dependence expected to be observed for a vortex medium consisting of noninteracting vortices (dashed line) and a vortex medium being dominated by bound vortex pairs (solid line). The Drude type of response has, in comparison to the MP form, a sharper transition between the high- and low-frequency limits of the frequency response. Comparing to experimental results, it can be seen that the  $fS_\phi(f)$  data for the 200 Å thick film [Fig. 8(a)], except for frequencies  $f/f_0(T) \gg 1$ , reasonably well follows the prediction of the MP form. The comparison for the 500 Å thick film is visualized in Fig. 8(b), and for this sample the transition between the high- and low-frequency limits of the frequency response is sharper and therefore the vortex dynamics for this film is better described by the Drude type of response or a mixture

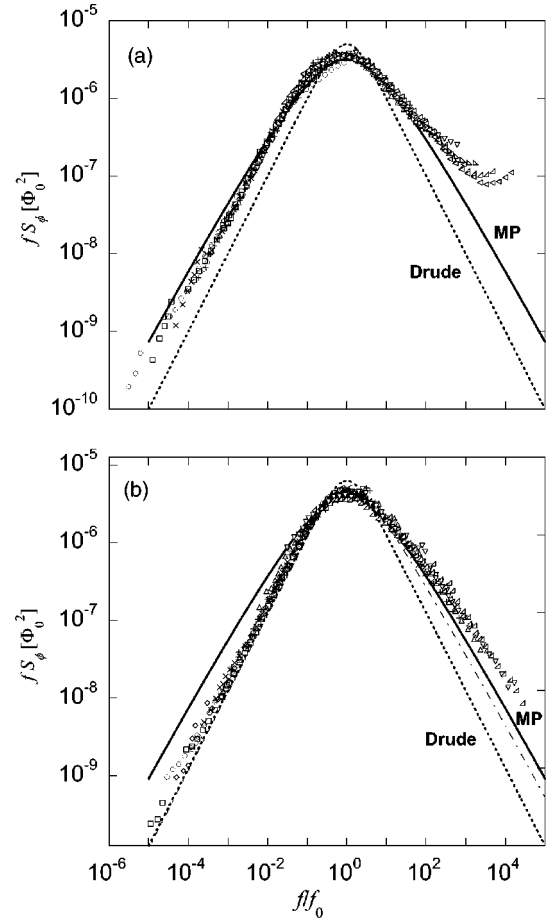


FIG. 8.  $fS_\phi$  versus frequency. (a) 200 Å thick film and (b) 500 Å thick film. Dashed and solid lines give the expected frequency response for a 2D superconductor following the Drude and MP response forms, respectively. The result for  $\chi''(f)$  calculated in Ref. 26, Eq. (20), for a superconducting disk is indicated by the dash-dotted line in (b).  $H_{dc} = 0$  Oe.

of the Drude and MP response functions. In particular, there is no clear sign of a logarithmic broadening of the frequency response, which according to the MP response form should be noticeable for frequencies  $f/f_0(T) \ll 1$ . However, the observed behavior for the 500 Å thick film can be explained considering in detail how flux-noise spectra measured at different temperatures contribute to the scaling plots shown in Fig. 8. Flux-noise spectra measured at high temperatures will primarily trace out the frequency dependence at  $f/f_0(T) \ll 1$ , while the main contribution at  $f/f_0(T) \gg 1$  originates from flux-noise measurements performed at low temperatures.

The peak ratio  $\chi''(f)/\chi'(f)$ , defined at the temperature where  $\chi''(f)$  exhibits a maximum, should take a value in the range  $2/\pi$  to 1;<sup>15</sup> according to the MP response form the peak ratio equals  $2/\pi$ , while a Drude type of response corresponds to a peak ratio of 1. For the present two samples, the peak ratio is close to  $2/\pi$  at the lowest frequency (lowest temperature), while the peak ratio increases for higher frequencies (higher temperatures). In accord with the results displayed in Fig. 8, the deviation of the peak ratio from the MP value is, comparing with the 200 Å thick film, more distinct for the 500 Å thick film, and the onset of an increas-

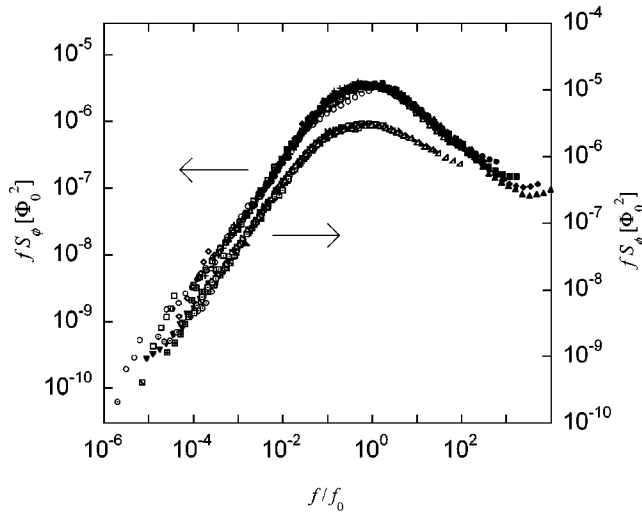


FIG. 9.  $fS_\phi$  versus frequency. The different scaling curves correspond to  $H_{dc}=0$  Oe (left-hand scale) and  $H_{dc}=1$  Oe (right-hand scale). 200 Å thick film.

ing peak ratio occurs at a lower frequency for this film. Moreover, for the highest frequency, the peak ratio for the 200 Å thick film takes a value well below the lower limit set by the MP response form, giving another indication of the heterogeneity of this film.

Brandt<sup>25,26</sup> calculated the electromagnetic response of thin strip- and disk-shaped superconductors to uniform applied perpendicular ac fields. In the Ohmic response regime he constructed, from the correct asymptotic behaviors at  $f/f_0 \gg 1$  and  $f/f_0 \ll 1$ , analytic expressions for the complex ac susceptibility that compared to a high degree of precision with the numerical solutions. The analytic expression constructed by Brandt for  $\chi''(f)$  exhibits a frequency dependence that coincides with the Drude frequency dependence at  $f/f_0 \ll 1$ , while at  $f/f_0 \gg 1$  the frequency dependence is broadened by a logarithmic frequency contribution of geometric origin; the frequency dependence of  $\chi''$  will at frequencies  $f/f_0 \gg 1$  follow a curve that falls between the frequency dependence of the Drude and MP response forms [cf. Fig. 8(b)]. Thus, the broadening of the frequency dependent response observed at  $f/f_0 \gg 1$  for the present two samples may to some extent be explained as being due to the experimental geometry.

In Fig. 9, the scaling result for the 200 Å thick film in an applied dc magnetic field of 1 Oe is shown together with the corresponding zero-field scaling result. As can be seen in this figure, the  $f/f_0$  scaling works as well in weak dc fields as it does in the zero-field limit. One difference in the frequency dependent response, comparing the weak-field and zero-field cases, can however be discerned. The  $f^{-x}$  dependence for frequencies  $f/f_0(T) \gg 1$  changes such that  $x$  decreases in applied field; for an applied field of 1 Oe,  $x \approx 1.3$ , which should be compared to  $x \approx 1.55$  obtained for zero field. A similar decrease of  $x$  in applied field, was also observed for the 500 Å thick film, where  $x \approx 1.5$  in an applied field of 1 Oe ( $x \approx 1.75$  in zero field). The success of scaling of the  $fS_\phi(f)$  data, both in zero field and in weak applied perpendicular fields, shows that the frequency dependent response of the

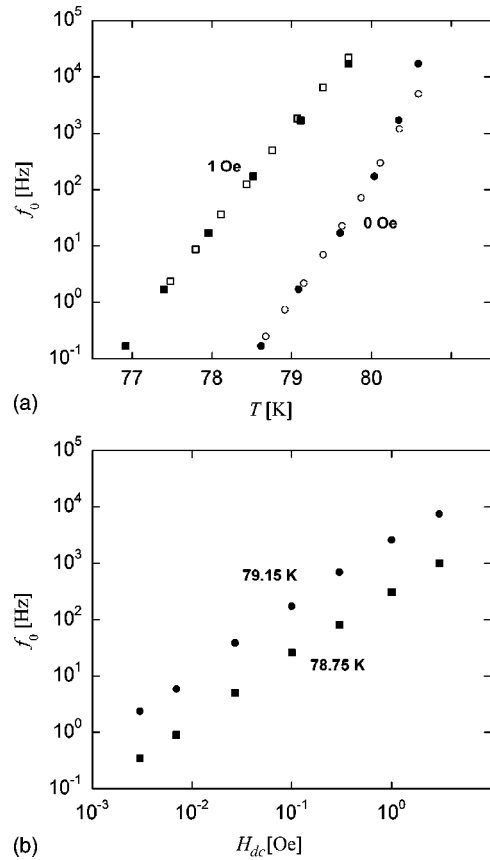


FIG. 10. (a) Characteristic frequency  $f_0$  versus temperature obtained from ac susceptibility (open symbols) and flux-noise (filled symbols) data. The different curves correspond to  $H_{dc}=0$  Oe and  $H_{dc}=1$  Oe. (b) Characteristic frequency  $f_0$  versus dc magnetic field  $H_{dc}$ . The different curves correspond to  $T=78.75$  K and  $T=79.15$  K. 200 Å thick film.

vortex medium is strongly temperature and field dependent, as described by  $f_0(T, H_{dc})$ , but that the general characteristics of the frequency dependence remain, despite the expected dominance of field-generated vortices in weak applied dc fields, the same throughout the transition region.

The characteristic frequency  $f_0(T)$  can be extracted from both flux-noise and ac susceptibility results. Plotting  $fS_\phi(f)$  versus  $f$ ,  $f_0(T)$  is defined as the frequency at which  $fS_\phi(f)$  obtains its maximum value. For temperatures where the frequency at which  $fS_\phi(f)$  obtains its maximum value is outside the experimental frequency range, it is still possible to estimate  $f_0(T)$  by carrying out the scaling analysis of the  $fS_\phi(f)$  data. Using instead the temperature dependence of  $\chi''$ , the frequency  $f$  of the ac field equals the characteristic frequency  $f_0$  at the temperature at which  $\chi''$  exhibits its maximum value. Figure 10(a) shows  $f_0$  vs  $T$ , including both magnetic flux-noise and ac susceptibility results, for zero dc field and a field of  $H_{dc}=1$  Oe for the 200 Å thick film. The characteristic frequency, in both the zero-field and weak-field cases, decreases by approximately five orders of magnitude in a temperature interval of 2 K, the main difference being that the  $f_0(T)$  curve corresponding to  $H_{dc}=1$  Oe is suppressed to lower temperature by  $\Delta T \approx 2$  K. Similar results were obtained for the 500 Å thick film. However, in concord with

the observation of a narrower transition for this sample,  $f_0$  decreases by five orders of magnitude in a temperature interval of only  $\approx 0.5$  K. Figure 10(b) shows  $f_0$  vs  $H_{dc}$ , for two different temperatures, for the 200 Å thick film. The magnitude of  $f_0$  increases by more than three orders of magnitude on increasing the applied field from the millioersted to the oersted range. In fact, the results indicate that the increase with field is more pronounced than a simple  $f_0 \propto H_{dc}$  relation would suggest; for the 200 Å thick film, it is possible to fit a  $H_{dc}^y$  dependence to the  $f_0(H_{dc})$  curves, with  $y \approx 1.15$ . The deviation from a simple linear relationship between the characteristic frequency and the applied dc field is even more pronounced for the 500 Å thick film.

In the case of a vortex medium exhibiting a Drude type of response, theory predicts<sup>14,15</sup> that  $f_0$  should be proportional to the density of free vortices  $n_F(T)$ . In case of the MP response, the prediction for a 2D vortex medium is rather that  $f_0$  is proportional to the total density of vortices (with the exception for temperatures being very close to the KT transition temperature, where instead  $f_0 \propto n_F$  is expected to hold). In the simplest case, one would thus expect  $f_0$  to be proportional to the applied field. Deviations from this linear dependence can be explained by an applied field dependent density of thermally created vortices, something that has also been observed in simulations of 2D vortex dynamics on *XY*-type models with Ginzburg-Landau dynamics.<sup>14,15</sup> In fact, one may argue that the experimental observation of an approximate  $f_0 \propto H_{dc}^{1.15}$  dependence for the 200 Å thick film indicates that thermally created as well as field-generated vortices contribute to the observed field dependent effects. The situation can be described as follows. The Coulomb gas temperature  $T^{CG} \propto T/\rho_0$ , where  $\rho_0$  is the superfluid density, increases with increasing applied dc magnetic field, and as a consequence, apart from an increase in field-generated vortices, one also expects an increase in the density of thermally created vortices with increasing field.

In Fig. 11(a), the dc resistance  $R$  as given by the inverse of the zero-frequency limit of  $S_\phi(f)$  is plotted for the 200 Å thick film as a function of dc magnetic field for two different temperatures. The resistance exhibits a very similar field dependence as does  $f_0$ . This is expected, since the resistance should exhibit a linear dependence on the density of free vortices  $n_F$ . To emphasize the simple linear relationship between the resistance and the characteristic frequency, Fig. 11(b) shows  $R$  versus  $f_0$ . This linear relationship holds both at constant temperature on varying the dc field and at constant dc field on varying the temperature.

## V. CONCLUDING REMARKS

In the present paper, we have presented results from two-coil mutual inductance and flux noise measurements close to the resistive transition of YBCO thin films. The experimental results give a detailed account of the zero-field vortex dynamics over six decades of frequency and how it develops with temperature on approaching the resistive transition from above, as well as describing the effects of weak applied dc fields. The frequency dependent linear response of the vortex medium is to a large extent governed by a strongly tempera-

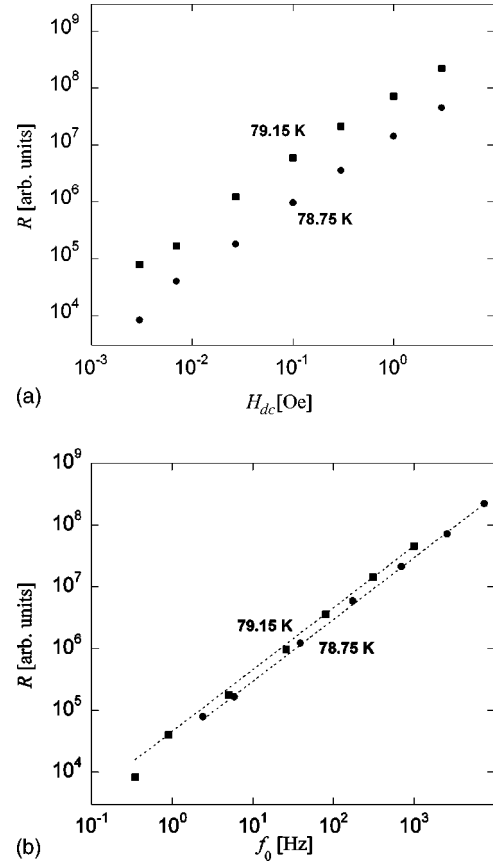


FIG. 11. (a) Resistance  $R$  versus dc magnetic field  $H_{dc}$ . The different curves correspond to  $T=78.75$  K and  $T=79.15$  K. (b) Resistance  $R$  versus characteristic frequency  $f_0$ . The different curves correspond to  $T=78.75$  K and  $T=79.15$  K. The dashed lines mark a fit of the experimental data to  $R=Cf_0$ , where  $C$  is a temperature dependent constant. 200 Å thick film.

ture and field dependent characteristic frequency  $f_0(T, H_{dc})$ , and the detailed frequency dependence of the vortex dynamics can be described as a mixture of a Drude type of response and the MP response. Deviations in the frequency response for frequencies  $f \gg f_0$ , comparing experimental results with the theoretical prediction of a  $f^{-2}$  dependence, can to a large extent be explained by imperfect sample quality. For a high- $T_c$  film close to the resistive transition, the important sample heterogeneity corresponds to oxygen deficiency. The field dependence of the characteristic frequency is found to approximately follow an  $H_{dc}^y$  dependence, with  $y \approx 1.15$ , indicating a vortex medium consisting of both thermally and field created vortices. Lastly, a simple linear relationship is found between  $f_0(T, H_{dc})$  and the resistance  $R(T, H_{dc})$ , where  $R$ , at constant temperature and dc magnetic field, is determined as the inverse of the zero-frequency limit of the noise spectrum.

## ACKNOWLEDGMENTS

The authors would like to thank H. Jeldtoft Jensen, P. Minnhagen, and H. Weber for interesting discussions. This work was supported by the Swedish Research Council.



- <sup>1</sup>P. Minnhagen, Rev. Mod. Phys. **59**, 1001 (1987).
- <sup>2</sup>C.T. Rogers, K.E. Myers, J.N. Eckstein, and I. Bozovic, Phys. Rev. Lett. **69**, 160 (1992).
- <sup>3</sup>Ö. Festin, P. Svedlindh, B.J. Kim, P. Minnhagen, R. Chakalov, and Z. Ivanov, Phys. Rev. Lett. **83**, 5567 (1999).
- <sup>4</sup>J. Kötzler, D. Görnitz, S. Skwirblies, and A. Wriedt, Phys. Rev. Lett. **87**, 127005 (2001).
- <sup>5</sup>T.J. Shaw, M.J. Ferrari, L.L. Sohn, D.-H Lee, M. Tinkham, and J. Clarke, Phys. Rev. Lett. **76**, 2551 (1996).
- <sup>6</sup>S. Candia, Ch. Leemann, S. Mouaziz, and P. Martinoli, Physica C **369**, 309 (2002).
- <sup>7</sup>D.P. Norton and D.H. Lowndes, Phys. Rev. B **48**, 6460 (1993).
- <sup>8</sup>J.M. Repaci, C. Kwon, Q. Li, X. Jiang, T. Venkatesan, R.E. Glover, C.J. Lobb, and R.S. Newrock, Phys. Rev. B **54**, R9674 (1996).
- <sup>9</sup>Ö. Festin, P. Svedlindh, A. Rydh, and P. Minnhagen (unpublished).
- <sup>10</sup>P. Minnhagen and P. Olsson, Phys. Rev. Lett. **67**, 1039 (1991).
- <sup>11</sup>S.W. Pierson, Phys. Rev. Lett. **73**, 2496 (1994).
- <sup>12</sup>A.T. Fiory and A.F. Hebard, Phys. Rev. B **25**, 2073 (1982).
- <sup>13</sup>R. Theron, J.-B. Simond, Ch. Leemann, H. Beck, P. Martinoli, and P. Minnhagen, Phys. Rev. Lett. **71**, 1246 (1993).
- <sup>14</sup>A. Jonsson and P. Minnhagen, Physica C **277**, 161 (1997).
- <sup>15</sup>A. Jonsson and P. Minnhagen, Phys. Rev. B **55**, 9035 (1997).
- <sup>16</sup>F. Rönnung, Ph.D. thesis, Chalmers University of Technology, 2003.
- <sup>17</sup>Ö. Festin and P. Svedlindh (unpublished).
- <sup>18</sup>J. Magnusson, C. Djurberg, P. Granberg, and P. Nordblad, Rev. Sci. Instrum. **68**, 3761 (1997).
- <sup>19</sup>B. Jeanneret, J.L. Gavilano, G.A. Racine, Ch. Leemann, and P. Martinoli, Appl. Phys. Lett. **55**, 2336 (1989).
- <sup>20</sup>M. Tinkham, *Introduction to Superconductivity* (McGraw-Hill, New York, 1975), p. 80.
- <sup>21</sup>B.J. Kim and P. Minnhagen, Phys. Rev. B **60**, 6834 (1999).
- <sup>22</sup>V. Ambegaokar, B.I. Halperin, D. Nelson, and E.D. Siggia, Phys. Rev. Lett. **40**, 783 (1978); Phys. Rev. B **21**, 1806 (1980).
- <sup>23</sup>Ö. Festin, P. Svedlindh, and Z. Ivanov, Physica B **284–288**, 963 (2000).
- <sup>24</sup>J. Houlrik, A. Jonsson, and P. Minnhagen, Phys. Rev. B **50**, 3953 (1994).
- <sup>25</sup>E.H. Brandt, Phys. Rev. B **49**, 9024 (1994); **50**, 4034 (1994).
- <sup>26</sup>E.H. Brandt, Phys. Rev. B **50**, 13 833 (1994).